RESEARCH ARTICLE

The effects of cultivated ginseng on rhizosphere microbial community structure and its interaction with pathogenic bacteria

Xiaohua Wu*

School of Medicine, Nanchang Institute of Technology, Nanchang, Jiangxi 330044, China.

Received: September 19, 2025; **accepted:** January 16, 2026.

Ginseng as a precious traditional Chinese medicinal herb has been cultivated for over 400 years. To explore the suitable soil types for cultivating ginseng and improve its yield, this study analyzed the effects of cultivating ginseng on the structure of rhizosphere microbial community (RMC) and the mechanisms of its interaction with pathogens. The study analyzed the composition and diversity of the RMC in ginseng under different cultivation conditions using next-generation sequencing technology. The results demonstrated that cultivating ginseng altered the RMC structure, increased the abundance of beneficial microorganisms, and inhibited the growth of pathogenic bacteria. The enrichment of prokaryotic microorganisms in rhizosphere soil (RS) resulted in inhibition rates of 76.9 ± 3.2% and 89.2 ± 3.7% against *Cylindropon destructants* and *Rhizoctonia solani*. The pH value of RS was generally lower than that of non-RS, and correlation matrix analysis showed significant ecological connections and synergistic effects between RS microbial communities. Cultivating ginseng significantly altered the RMC structure, optimized the abundance of beneficial microorganisms, and had a significant inhibitory effect on pathogenic bacteria. Therefore, by regulating the RMC structure, it is expected to improve the disease resistance and yield of ginseng.

Keywords: ginseng; rhizosphere microbial community; pathogenic bacteria; high-throughput sequencing.

***Corresponding author:** Xiaohua Wu, School of Medicine, Nanchang Institute of Technology, Nanchang, Jiangxi 330044, China. Email: jxnc_123456@126.com.

Introduction

Ginseng C.A. Meyer is a precious traditional Chinese medicine with a cultivation history of over 400 years. It has long been widely used in Asian countries to treat various symptoms, and its medicinal value and economic importance have been widely recognized in traditional medicine and modern pharmaceutical research [1]. In the soil plant system, the rhizosphere microbial community (RMC) is an important component involved in various key ecological processes such as soil material cycling, nutrient transformation, and pest control, which plays an irreplaceable role in regulating plant growth, development, and health status [2, 3].

With the deepening of research on ginseng cultivation and soil microbiology, researchers have made certain progress in related fields. Fan *et al*. analyzed the land suitability of ginseng planting by studying the method of simulating ginseng planting in the wild. The proportion of soil suitable for planting ginseng was found to be less than 50%, and planting in suitable soil also showed a low yield increase rate with a gradually slow trend of increasing production [4]. In nature, the soil environment plays a crucial role in plant

growth [5]. Therefore, studying these components is of great significance for finding soil nutrients suitable for ginseng's growth. The RMC is a vital component of the soil plant system, which participates in various ecological processes such as soil material cycling, nutrient transformation, and pest control. It is essential for the growth, development, and health status of plants [6]. Chen *et al*. studied the physicochemical properties and RMC soil when planting American ginseng in China and found that changes in RMC soils of different age groups caused soil-borne diseases [7]. Jang *et al*. utilized high-throughput sequencing technology (HTST) to analyze ginseng's genes, validating the effectiveness of this technology as a molecular breeding tool [8]. In addition, soil environment is a key factor affecting plant growth. The interaction between RMC and plants is one of the core topics in current agricultural and environmental microbiology research. Despite research progress, ginseng cultivation still faces prominent issues that urgently need to be addressed. With the continuous increase in demand for ginseng in the market, its planting area and scale continue to expand. However, long-term intensive soil planting has led to a significant decrease in soil organic matter content and weakened soil fertility, resulting in low ginseng yield and increasingly serious pest and disease problems. The traditional methods of ginseng cultivation include deforestation, understory planting, and field planting with the first two methods unable to achieve large-scale production due to ecological limitations and low efficiency, while field planting leads to further yield decline, and continuous cropping cannot be carried out due to soil nutrient degradation. Meanwhile, the relationship between the RMC structure of ginseng and pathogenic bacteria, as well as the driving factors of RMC changes, is still unclear, which further restricts the development of efficient and sustainable ginseng cultivation techniques.

This study explored suitable soil types for ginseng cultivation by elucidating the differences in RMC structure and soil physicochemical properties between ginseng rhizosphere soil (RS) and non-rhizosphere soil (NRS), analyzed the impact of ginseng cultivation on RMC structure, investigated the interaction mechanism between ginseng RMC and pathogenic bacteria, and identified the key factors suitable for ginseng cultivation to provide scientific basis for solving the problems of ginseng yield reduction and disease, and promote healthy cultivation of ginseng. This study theoretically elucidated the directional selection effect of ginseng cultivation on RMC, revealing the coupling relationship between soil physicochemical properties and RMC structure, filling the research gap in the interaction mechanism between ginseng RMC and key pathogens. Further, the research results provided a scientific basis for regulating the RMC structure to improve the disease resistance and yield of ginseng, which could help to address low yield, severe diseases, and difficulty in continuous cropping in ginseng cultivation and promote the development of sustainable and healthy ginseng cultivation technology.

Materials and methods

Experimental location

The experimental site was in Fusong, Baishan, Jilin, China with geographical coordinates of 128°25’55” E and 42°49’30” N in the western foothills of Changbai Mountain at an altitude of about 697 m [9, 10]. The ginseng was cultivated in a standardized ginseng planting base. The study region belongs to a temperate continental humid monsoon climate with significant mountainous climate characteristics. The main climatic characteristics are dry and windy in spring, warm, humid, and rainy in summer, cool and brief in autumn, and long, cold, and dry in winter [11]. The annual mean temperature is about 3-4°C, and the annual average precipitation is about 800 to 900 mm, mainly concentrated from June to August.

Sample plot setting

The sample plot for cultivating ginseng was selected from a fallow land. A total of 5 parallel

planting plots were set up in the experimental area, numbered Y1-Y5, to ensure experimental repeatability and data reliability. Among them, plot Y5 was the key monitoring plot, located in the middle of the experimental area with an area of 20 m × 15 m. Its soil pretreatment and planting management measures were completely consistent with other plots, and it was used for subsequent pathogen isolation experiments. Lime (Shandong Sinochem Chemical Co., Ltd., Jinan, Shandong, China) was first used to adjust the pH of the soil to about 6.0. Before cultivating the land, 50% carbendazim and 3% phoxim (Jiangsu Changqing Agrochemical Co., Ltd., Changzhou, Jiangsu, China) were used to disinfect the soil to kill pests and insect eggs [12, 13]. Subsequently, fully decomposed organic fertilizers (Genlidao Biotechnology Co., Ltd., Xingtai, Hebei, China) were mixed and ginseng seeds that had already germinated were sown on demand. The sowing row spacing was set to 5 cm × 5 cm. After sowing, a 5 cm thick layer of soil was covered with a layer of deciduous leaves of *Quercus mongolica* on top of the soil, which was a common broad-leaved tree species in the Changbai Mountain area, and its leaves had a moderate decomposition rate to balance the needs of soil moisture retention and organic matter supplementation.

Sample collection

The soil samples were collected from the ginseng cultivation site. A random sampling method was utilized to collect 5 samples of ginseng at each sampling point for testing. Then, NRS samples were collected utilizing shaking method and labeled as A1 to A5. Sterile spatulas were taken to collect RS attached to the roots of the samples and labeled as B1 to B5. All collected samples were stored in sterile sealed bags. The samples for microbial community analysis were stored in a -80℃ freezer, while the samples used for measuring soil physicochemical properties and other related indicators were left to air dry naturally at room temperature.

Soil physical and chemical property tests

(1) Organic matter detection

Potassium dichromate oxidation method was employed to detect organic matter. After passing through a 100-mesh sieve, 0.5 g air-dried soil sample was placed in a digestion tube followed by adding 5 mL of 0.8 mol/L potassium dichromate and 5 mL of 98% H_2SO_4 (Sinopharm Chemical Reagent Co., Ltd., Shanghai, China). After gentle mixing, the tube was placed in Labtech ETHO-420 intelligent temperature-controlled digestion instrument (Beijing Labtech Instrument Co., Ltd., Beijing, China) and digested at 170-180℃ for 5 min. After digestion, the tube was cooled to room temperature, 20 mL distilled water was added, and the mixture was transferred to a 250 mL Erlenmeyer flask. After adding 3 drops of phenanthroline indicator, the solution was titrated with 0.2 mol/L ferrous sulfate solution until the color changed from orange-red to brick-red. The volume of ferrous sulfate consumed was recorded, and the organic matter content was calculated.

(2) Soil pH value determination

The potentiometric method (soil:water = 1:2.5) was used to determine soil pH value. After passing through a 2-mm sieve, 10 g air-dried soil sample was placed in a 50 mL centrifuge tube, and 25 mL carbon dioxide-free distilled water was added. The mixture was shaken at 25℃ and 180 rpm for 30 min in a THZ-82 reciprocating shaker (Jintan Dadi, Changzhou, Jiangsu, China), then left to stand for 30 min to separate layers. The pH was measured using Leici PHS-3E pH meter (Shanghai Yidian Scientific Instruments Co., Ltd., Shanghai, China).

(3) Determination of total nitrogen content

Kjeldahl method was employed to determine soil total nitrogen content. After passing through a 100-mesh sieve, 1 g air-dried soil sample was placed in a digestion tube followed by adding 5 g catalyst mixed by K_2SO_4 and $CuSO_4{\cdot}5H_2O$ at a mass ratio of 10:1 and 10 mL of 98% H_2SO_4. The tube was placed in the digestion module of a FOSS Kjeltec 8400 Automatic Kjeldahl Nitrogen Analyzer (FOSS Analytical Instruments (Suzhou) Co., Ltd., Suzhou, Jiangsu, China) and digested at 420℃ for 2 h until the solution turned clear blue

green. After cooling, the digestion tube was moved to the distillation module, and 30 mL of 40% NaOH solution was added for 5 min distillation. The distillate was collected with 20 mL of 2% boric acid absorption solution and titrated with 0.05 mol/L HCl standard solution until the color changed from blue green to pink. The total nitrogen content was calculated based on the volume of HCl consumed.

(4) Determination of available phosphorus content

Molybdenum antimony blue colorimetric method was used for the sodium bicarbonate extraction. Briefly, after passing through a 2-mm sieve, 5 g of air-dried soil sample was mixed with 100 mL of 0.5 mol/L $NaHCO_3$ solution and shaken at 25℃, 180 rpm, for 30 min before being filtered with quantitative filter paper. A total of 5 mL filtrate was then mixed with 5 mL of molybdenum antimony anti-color reagent pre-prepared by mixing 10 mL of 5% ammonium molybdate solution and 10 mL of 0.15% potassium antimonyl tartrate solution with 100 mL of 0.5 mol/L H_2SO_4 and 0.5 g ascorbic acid. The solution was left to stand in the dark for 30 min for color development. The absorbance at 660 nm was measured using a Shimadzu UV-1800 UV-visible spectrophotometer (Shimadzu Corporation (China) Co., Ltd., Shanghai, China). The available phosphorus content was calculated using the phosphorus standard curve.

(5) Determination of alkali-hydrolyzable nitrogen content

2 g air-dried soil sample was placed in the outer chamber of the 9 cm alkali hydrolysis diffusion dish, while 2 mL of 2% boric acid absorption solution was added to the inner chamber. Alkaline glycerol was evenly applied to the edge of the diffusion dish followed by adding 10 mL of 1.0 mol/L NaOH solution. The diffusion dish was placed in a DHP-9052 constant temperature incubator (Shanghai Yiheng, Shanghai, China) at 40℃ for 24 h. After incubation, the absorption solution in the inner chamber was titrated with 0.01 mol/L HCl standard solution until the endpoint, and the alkali-hydrolyzable nitrogen content was analyzed using a FOSS Kjeltec 2300 Semi-Automatic Kjeldahl Nitrogen Analyzer (FOSS A/S, Hillerød, Denmark) and calculated based on the volume of HCl consumed.

(6) Determination of available potassium content

5 g air-dried soil sample was mixed with 50 mL of 1.0 mol/L NH_4OAc solution and shaken at 25℃, 180 rpm, for 30 min before centrifugation at 4,000 rpm for 10 min. The supernatant was introduced into Sherwood M410 Flame Photometer (Sherwood Scientific Ltd., Cambridge, Cambridgeshire, UK) with acetylene-air flame as the excitation source and acetylene flow rate of 0.5 L/min, air flow rate of 5 L/min to measure the potassium emission intensity at 766.5 nm. A standard curve was plotted using the potassium standard series of 0, 10, 20, 40, 60, and 80 μg/mL. The available potassium content was calculated by substituting the sample emission intensity into the curve.

Microbial community analysis

Total soil DNA was extracted using MoBio PowerOil®DNA extraction kit (QIAGEN, Valencia, California, USA) following the manufacturer's instructions. The V3-V4 region of bacterial 16S rRNA was selected for PCR amplification utilizing primers 338F (5'-ACT CCT ACG GGA GGC AGC AG-3') and 806R (5'-GGA CTA CHV GGG TWT CTA AT-3'), while ITS1 region of fungi was used with the primers ITS5F (5'-GGA AGT AAA AGT CGT AAC AAG G-3') and ITS1R (5'-GCT GCG TTC TTC ATC GAT GC-3'). The PCR products were then subjected to HTST to analyze the microbial community of soil using Illumina PE250 NovaSeq platform (Illumina, San Diego, California, USA) with a sequencing quantity of no less than 50,000 sequences per sample [14]. The sequencing results were analyzed using QIIME2 (University of California, Berkeley, CA, USA), which first used Denoising Algorithm 2 (DADA2) to denoise followed by utilizing Silva (https://www.arb-silva.de/) and UNITE database (https://unite.ut.ee/) for classification. The analysis of α-diversity and β-diversity was conducted using Shannon index and principal

coordinates analysis (PCoA). To further compare the number and relative abundance of operational taxonomic units (OTUs) between prokaryotic microorganisms (PMG) and eukaryotic microorganisms (EMG) in NRS and RS samples, a rank abundance curve was plotted for statistical analysis.

Isolation and interaction verification of pathogenic bacteria

This study isolated *Cylindrocarpon* destructants and *Rhizoctonia solani* from typical diseased roots of Y5 plot in PDA medium (Beijing Solarbio Science & Technology Co., Ltd., Beijing, China) at 25℃. The plate confrontation method was used for antagonistic experiments. Briefly, *Bacillus* and *Pseudomonas* genera (China General Microbiological Culture Collection Center, Beijing, China) were selected from the differentially enriched bacterial communities for pure cultivation. The strain points were inoculated onto the edge of the pathogen plate, and the diameter of the inhibition zone was measured 72 hours later. The antibacterial rate was calculated as follows.

$$I = \frac{D_c - D_t}{D_c} \times 100\% \quad (1)$$

where I was the inhibition rate. D_c and D_t were the colony diameters of the control and the treatment groups.

Data processing

RDP classifier Bayesian algorithm (Center for Microbial Ecology, Michigan State University, East Lansing, MI, USA) was employed to carry out taxonomic analysis on OTU representative sequences with 97% similarity level. R language was used to create curve graphs [15]. The differences in community structure were tested using PERMANOVA, and the correlation between microorganisms and physicochemical factors was explored through Spearman analysis. Gephi software (Institut National de Recherche en Informatique et en Automatique (INRIA), France) was used to draw alpha and beta diversity maps and network diagrams. The data were analyzed by using SPSS 24.0 (IBM, Armonk, New York, USA) and SAS 9.4 software (SAS, Cary, NC, USA) with a *P* value less than 0.05 as statistically significant.

Results

RMC structure

The microbial rank abundance curves in soil were compared to analyzing the structural characteristics of RMC. The results showed that the OTU numbers of PMG A1 to A5 in NRS samples ranged from 1,300 to 3,600 with relative abundances ranging from -4.5 to -5.0 (log10). The amount of eukaryotic microbial OTUs in NRS samples ranged from 500 to 1,000 with a relative abundance of -5.0 to -5.5 (log10) (Figure 1a). Further, the OTU numbers of PMG from B1 to B5 in the RS samples ranged from 1,100 to 2,400 with relative abundances ranging from -4.5 to -5.0 (log10). The number of eukaryotic microbial OTUs in RS samples ranged from 600 to 900 with a relative abundance in the range of -5.0 to -5.5 (log10) (Figure 1b). The amount and relative abundance of PMG OTUs in NRS were higher than those in RS. The difference in OTU quantity and relative abundance of EMG in RS and NRS was relatively small. The results suggested that the number and abundance of microorganisms in NRS were superior to those in RS. The comparison results of α-diversity of RMC in soil demonstrated that, in terms of PMG, the Chao1 index of NRS was 3,246.15 ± 185.23, which was significantly higher than that of RS at 2,018.20 ± 153.64 ($P < 0.001$) with an increase of 37.82% in species richness index. The ACE index for NRS was 3,357.61 ± 192.89, while for RS it was 2,125.28 ± 167.21. NRS was significantly higher than RS ($P < 0.05$) with an increase of 36.69%. In terms of species diversity indicators, the Shannon index of NRS was 9.42 ± 0.35, which was significantly higher than that of RS at 8.15 ± 0.28 by 15.60% ($P < 0.01$). The Simpson (1-D) index for NRS was 0.982 ± 0.008, which was also higher than the 0.953 ± 0.012 for RS ($P < 0.05$) with an increase of 3.04%. In terms of the phylogenetic diversity index PDw_hole_tree, the NRS score was 85.35 ± 3.62, significantly higher than the RS

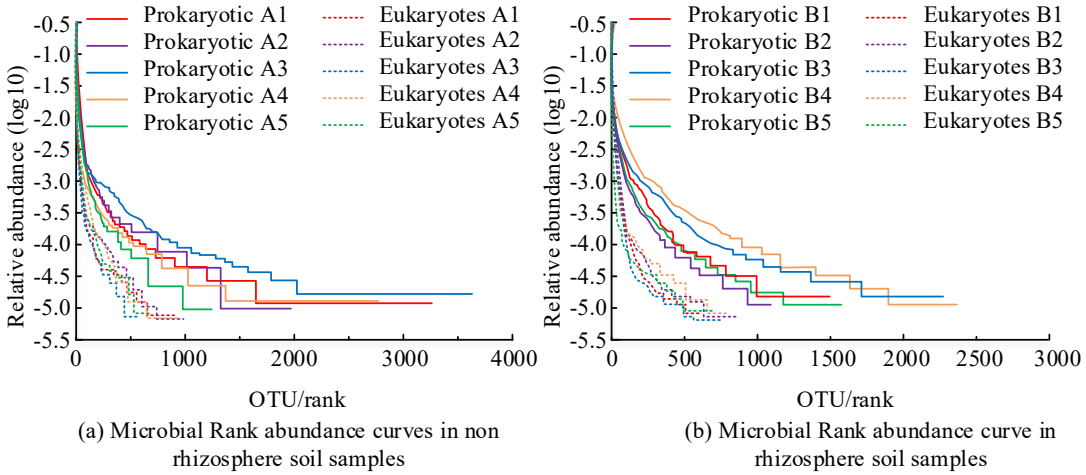

Figure 1. Comparison of rank abundance curves of microorganisms in soil.

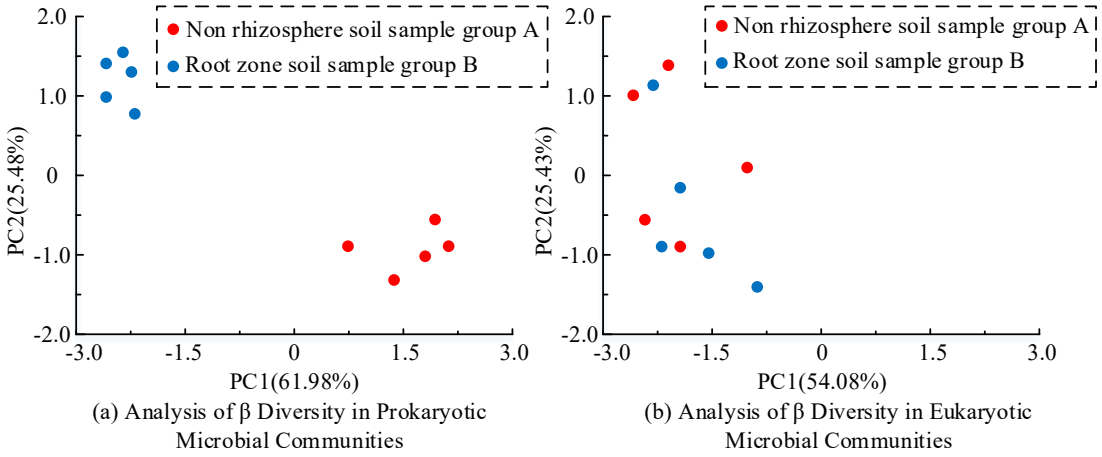

Figure 2. Comparison of β diversity of rhizosphere microbial communities in soil.

score of 63.74 ± 4.20 ($P < 0.001$) with an increase of 33.80%. In terms of EMG, the Chao1 index for species richness indicators was 872.65 ± 64.25 for NRS and 798.64 ± 71.09 for RS, respectively, with no significant difference being observed. The ACE index for NRS was 905.64 ± 58.47, while it was 823.58 ± 62.28 for RS with no significant difference. In terms of species diversity indicators, the Shannon index of RS was 6.52 ± 0.37, significantly higher than that of NRS at 5.87 ± 0.41 ($P < 0.05$). The Simpson (1-D) index was 0.861 ± 0.022 for NRS and 0.892 ± 0.019 for RS with no significant difference between the two groups. The phylogenetic diversity index PDw_hole_tree was 32.20 ± 2.89 for NRS and 30.54 ± 3.15 for RS with no significant difference. The results confirmed that the alpha diversity of PMG in RS was significantly lower than that in NRS, while there was no significant difference in alpha diversity of EMG. The comparison of beta diversity of RMC in soil showed that the distribution of RS and NRS samples was significantly different in the β-diversity analysis of prokaryotic microbial communities (PMC). The PC1 values of group A samples in NRS were all positive, while the PC1 values of group B samples in RS were all negative. The variances of PC1 and PC2 were 61.98% and 25.48%, respectively, which indicated that the PC1 axis explained 61.98% of bacterial community changes,

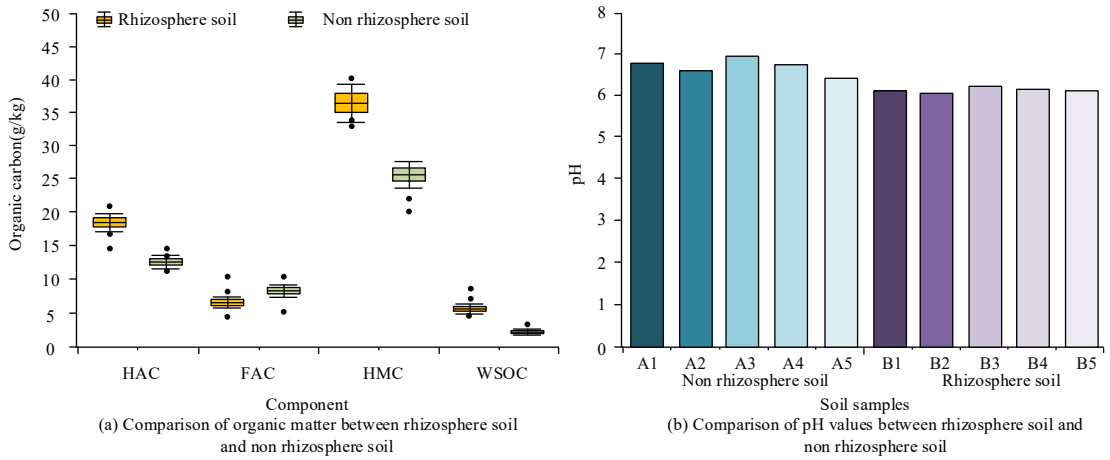

Figure 3. Comparison of organic matter and pH values between RS and NRS.

demonstrating significant differences in PMC structure between RS and NRS. PC2 explained 25.48% of the changes, further supporting the significant separation in community structure between RS and NRS sample groups (Figure 2a). The PC1 axis explained 54.08% of the variation in the beta diversity analysis of Eukaryotic Microbial Communities (EMC), while the PC2 axis explained 25.43% of the variation (Figure 2b). The RS and NRS samples were focused on the negative area of the PC1 axis. Although the distance difference within each group of samples was not significant, overall, there were differences in the distribution of EMC in RS and NRS along the PC1 axis. There was a difference in the beta diversity of PMC between RS and NRS, while the beta diversity difference of EMC was not as significant as that of PMC. There were 8 groups enriched in RS in the PMC including *Actinobacteria*, *Firmicutes*, *Saccharimonadia*, *Bacillus*, *Xanthomonaales*, *Bacillales*, *Mizugakiibacter*, *Pullulanibacillus* and 3 types of prokaryotic groups enriched in NRS including *Gemmatimonas*, *Blastocatellia* Subgroup-4, and *Phycisphaerae*. In the EMC, there were 3 enriched groups in the RS as *Chaetomiaceae*, *Humicola, Humicola grisea* and 6 eukaryotic taxa enriched in NRS as *Dothideomycetes*, *Pleosporales*, *Didymosphaeriaceae*, *Bionnectriaceae*, *Necteriopsis*, *Zopfiella*. There were differences in the Microbial Community Structure (MCS) between RS and NRS, indicating that the rhizosphere environment in ginseng had a significant effect on the composition of microbial communities.

Soil physical and chemical properties

The comparative results of the organic matter and pH values in RS and NRS showed that the humic acid carbon (HAC), fulvic acid carbon (FAC), hu minsu carbon (HMC), water-soluble organic carbon (WSOC) in RS and NRS were 18.3 ± 1.5 and 12.5 ± 1.2 g/kg, 6.5 ± 0.7 and 8.2 ± 0.8 g/kg, 36.4 ± 2.8 and 25.7 ± 2.1 g/kg, 5.6 ± 0.6 and 2.1 ± 0.3 g/kg, respectively. The contents of HAC, HMC, and WSOC in RS was higher than that in NRS, while the content of FAC was higher in NRS (Figure 3a). The results of pH comparison showed that the pH values in the A1 to A5 sample groups of NRS were within the range of 6.52 - 6.91, while, in the B1 to B5 sample groups of RS, the pH value was within the 6.05 - 6.22, indicating that the pH value of RS was generally lower than that of NRS (Figure 3b). The organic matter content in RS was higher than NRS and the pH value was lower. The comparison of total nitrogen and alkali hydrolyzed nitrogen contents between RS and NRS showed that the total nitrogen content (TNC) in the A1 to A5 sample groups of NRS ranged from 1,795.5 ± 40.2 to 1,937.4 ± 45.6 g/kg, while the TNC in the B1 to B5 sample groups of RS ranged from 2,103.1 ± 46.0 to 2,316.4 ± 55.7

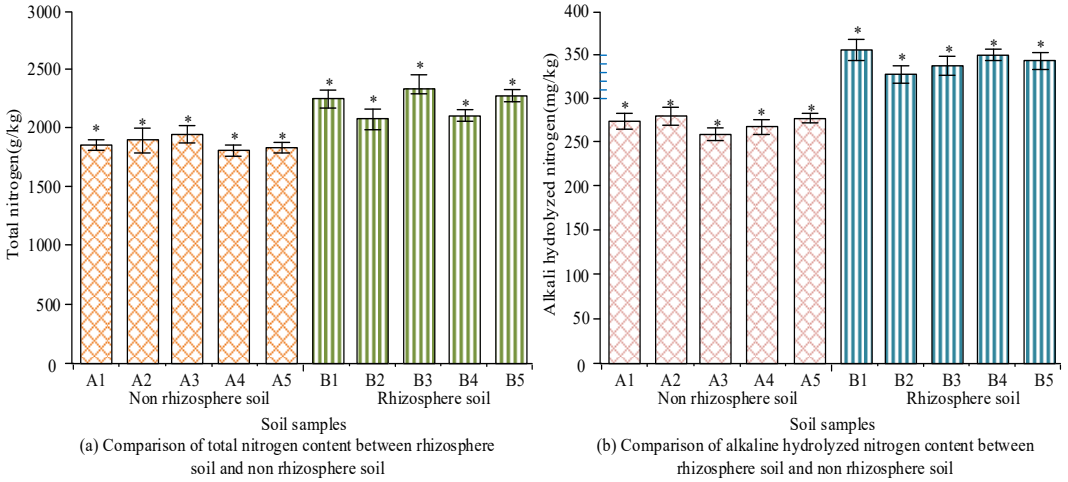

Figure 4. Comparison of total nitrogen and alkali hydrolyzed nitrogen contents between RS and NRS. *: $P < 0.05$.

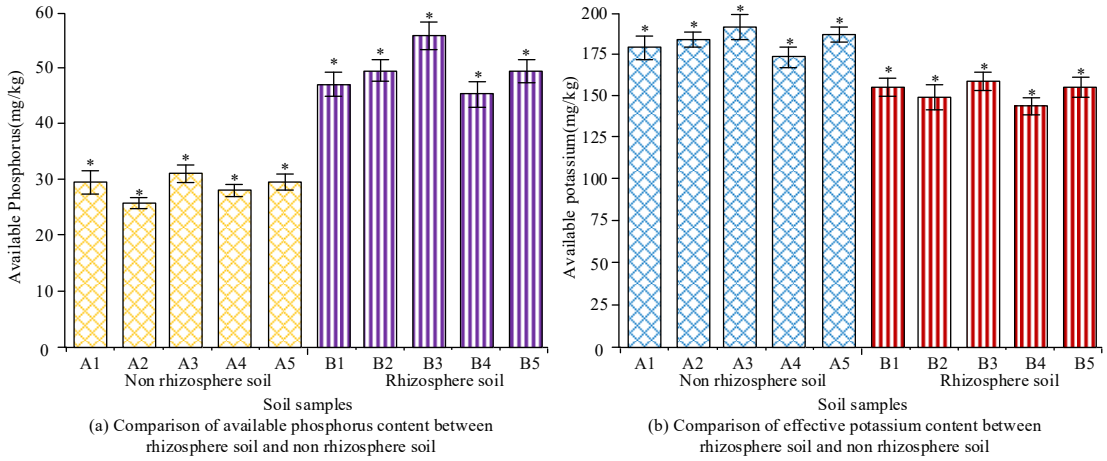

Figure 5. Comparison of available phosphorus and potassium content between RS and NRS. *: $P < 0.05$.

g/kg. The TNC of NRS decreased by at least 11.4% compared to that of RS ($P < 0.05$) (Figure 4a). The alkaline nitrogen content (ANC) in the A1 to A5 sample groups of NRS ranged from 259.8 ± 7.6 to 281.5 ± 9.3 mg/kg. The ANC in the B1 to B5 sample groups of RS ranged from 327.4 ± 11.3 mg/kg to 355.8 ± 12.6 mg/kg. The ANC in NRS decreased by at least 20.4% compared to that of RS ($P < 0.05$) (Figure 4b). The TNC and alkaline hydrolyzed nitrogen content in RS were higher. The comparison of available phosphorus and potassium content between RS and NRS showed that the effective phosphorus content (EPC) in the A1 to A5 sample groups of NRS ranged from 25.7 ± 1.1 to 31.2 ± 1.5 mg/kg. The EPC in the B1 to B5 sample groups of RS ranged from 45.7 ± 2.0 to 56.1 ± 2.6 mg/kg. The EPC in NRS decreased by at least 45.1% compared to that of RS ($P < 0.05$) (Figure 5a). The EPC in the A1 to A5 sample groups of NRS ranged from 173.5 ± 6.1 to 192.4 ± 7.2 mg/kg, while the EPC in the B1 to B5 sample groups of RS ranged from 143.9 ± 5.4 to 158.4 ± 6.0 mg/kg. The EPC in NRS increased by at least 9.5% compared to that of RS ($P < 0.05$) (Figure 5b). There were an enrichment of available phosphorus and a decrease in available potassium in the RS of ginseng.

The interaction between microbial communities and pathogenic bacteria

Table 1. The antagonistic effect of enriched microorganisms in RS.

Microbial type	Microbial community	Antibacterial zone diameter (mm)		Antibacterial rate (%)	
		Cylindrocarpon destructans	***Fusarium graminearum***	***Cylindrocarpon destructans***	***Fusarium graminearum***
Prokaryotic communities	*Actinobacteria*	16.2 ± 0.6	19.5 ± 0.8	65.0 ± 2.8	78.2 ± 3.3
	Firmicutes	14.8 ± 0.5	17.3 ± 0.7	59.3 ± 2.5	69.5 ± 2.9
	Bacilli	18.7 ± 0.7	22.6 ± 0.9	75.0 ± 3.1	85.8 ± 3.5
	Xanthomonadales	12.5 ± 0.5	15.1 ± 0.6	50.2 ± 2.1	60.5 ± 2.6
	Bacillales	19.3 ± 0.8	23.8 ± 1.0	76.9 ± 3.2	89.2 ± 3.7
	Mizugakiibacter	10.6 ± 0.4	13.2 ± 0.5	42.5 ± 1.8	53.0 ± 2.3
	Pullulanibacillus	13.4 ± 0.5	16.8 ± 0.7	53.7 ± 2.3	67.1 ± 2.8
Eukaryotes	*Chaetomiaceae*	9.8 ± 0.4	12.5 ± 0.5	39.1 ± 1.7	50.3 ± 2.1
	Humicola	8.5 ± 0.3	10.2 ± 0.4	34.1 ± 1.5	41.0 ± 1.8
	H. grisea	11.2 ± 0.5	14.6 ± 0.6	45.0 ± 1.9	58.6 ± 2.5

Table 2. Antagonistic effect of enriched microorganisms in NRS.

Microbial type	Microbial community	Antibacterial zone diameter (mm)		Antibacterial rate (%)	
		Cylindrocarpon destructans	***Fusarium graminearum***	***Cylindrocarpo n destructans***	***Fusarium graminearum***
Prokaryotic communities	Gemmatimonadetes	2.1 ± 0.2	3.5 ± 0.3	8.4 ± 0.5	14.1 ± 0.8
	Blastocatellia_subgroup_4	0.0 ± 0.0	0.0 ± 0.0	0.0 ± 0.0	0.0 ± 0.0
	Phycisphaerae	-1.8 ± 0.2	-2.5 ± 0.3	-7.2 ± 0.6	-10.0 ± 0.9
Eukaryotes	Dothideomycetes	-3.2 ± 0.3	-4.1 ± 0.4	-12.8 ± 1.1	-16.4 ± 1.4
	Pleosporales	-2.7 ± 0.3	-3.5 ± 0.3	-10.8 ± 0.9	-14.0 ± 1.2
	Didymosphaeriaceae	-1.5 ± 0.2	-1.9 ± 0.2	-6.0 ± 0.5	-7.6 ± 0.7
	Bionectriaceae	-4.5 ± 0.4	-5.8 ± 0.5	-18.0 ± 1.5	-23.2 ± 2.0
	Nectriopsis	-0.8 ± 0.1	-1.2 ± 0.2	-3.2 ± 0.3	-4.8 ± 0.4
	Zopfiella	-2.1 ± 0.2	-2.7 ± 0.3	-8.4 ± 0.7	-10.8 ± 0.9

Common root associated pathogens in ginseng include *Cylindrocarpon destructants* and *Rhizoctonia solani* [16]. To verify the interaction results between microbial communities and pathogens, this study analyzed the antagonistic effect of soil microbial communities on ginseng rhizosphere pathogens using significantly different microbial communities with high LDA scores in soil. The antagonistic effect of enriched microorganisms in RS demonstrated that various microorganisms in the RS exhibited certain antibacterial effects on both *Cylindropon destructants* and *Rhizoctonia solani*, but there were differences in the antibacterial effects among various types of microorganisms. Among PMG, *Bacillales* and *Bacilli* showed the most significant antibacterial effects against *Cylindrocarpon destructants* and *Rhizoctonia solani* with inhibition zone diameters of 19.3 ± 0.8 mm and 23.8 ± 1.0 mm, and inhibition rates of 76.9 ± 3.2% and 89.2 ± 3.7%, respectively. In EMG, *H. grisea* had relatively good antibacterial effects on *Cylindrocarpon destructants* and *Rhizoctonia solani* with inhibition zone diameters of 11.2 ± 0.5 mm and 14.6 ± 0.6 mm, and inhibition rates of 45.0 ± 1.9% and 58.6 ± 2.5%, respectively (Table 1). The enriched microbial communities of *Bacillales* and *Bacilli* in the RS exhibited significant antagonistic effects on *Cylindrocarpon destructants* and *Rhizoctonia solani.* The antagonistic effects of enriched microorganisms in NRS showed that the antagonistic effect of NRS enriched microorganisms on *Cylindropon destructants* and *Rhizoctonia solani* was generally weak and even exhibited negative antibacterial effects in some

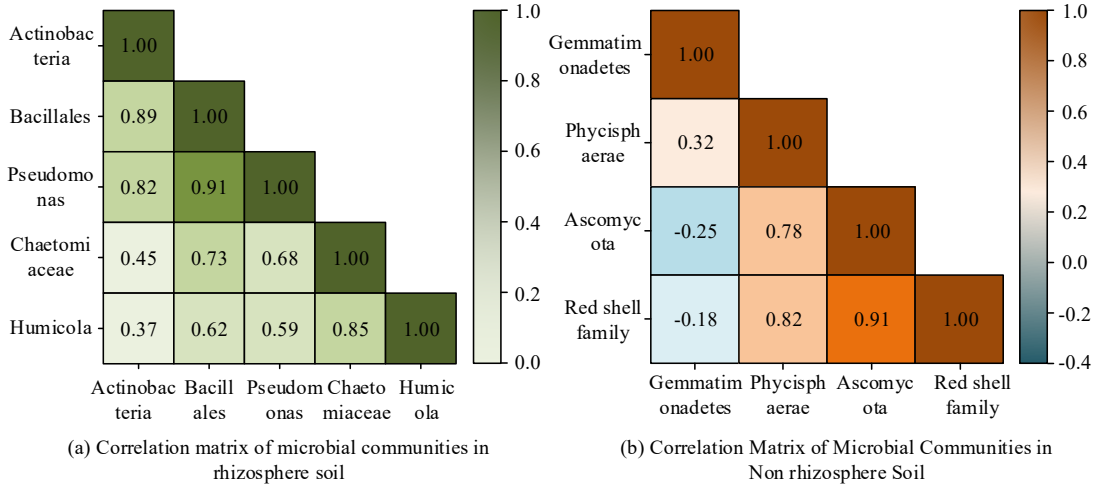

Figure 6. Correlation matrix of microbial communities in RS and NRS (|r|> 0.7, *P* < 0.01).

cases. In PMG, *Gemmatimonades* had relatively weak antibacterial effects on *Cylindrocarpon destructants* and *Rhizoctonia solani* with inhibition zone diameters of 2.1 ± 0.2 mm and 3.5 ± 0.3 mm, and inhibition rates of only 8.4 ± 0.5% and 14.1 ± 0.8%, respectively. Other PMG had no antibacterial effect and even had negative antibacterial effects on *Cylindrocarpon destructants* and *Rhizoctonia solani*. In EMG, all microbial communities exhibited negative antibacterial effects against pathogenic bacteria (Table 2). The microbial community enriched in NRS had a generally poor antagonistic effect on *Cylindropon destructants* and *Rhizoctonia solani*, and some microorganisms even exhibited negative antibacterial effects that promoted bacterial growth. In addition, the correlation between various groups in the RS microbial community was significant with the correlation coefficient between *Bacillales* and *Pseudomonas* reaching 0.91, showing a strong positive correlation. The correlation coefficient between *Bacillales* and *Chaetomiaceae* was 0.73, indicating a moderate positive correlation (Figure 6a). The correlation among NRS microbial communities was complex and not as close as that in RS microbial communities. The correlation coefficient between *Ascomycota* and the red shell family reached 0.91, indicating a strong positive correlation between them. However, the correlation between *Zygomycota phylum* and other microbial groups was weak, especially showing a negative correlation with *Ascomycota* and the red shell family (Figure 6b). The correlation between microbial communities in RS was stronger, while the correlation between microbial communities in NRS was more complex, and the connections between various groups were not as close as those in RS. The redundancy analysis of microbial communities and soil physicochemical factors demonstrated that, in the RDA analysis of PMC, the RDA1 axis explained 62.35% of the variation, mainly driven by organic matter and pH with organic matter showing a significant positive correlation and pH showing a negative correlation. The RDA2 axis explained 18.50% of the variation, mainly influenced by available phosphorus and available potassium with available phosphorus positively correlated and available potassium negatively correlated (Figure 7a). In the RDA analysis of EMC, the RDA1 axis explained 58.72% of the variation, mainly driven by organic matter and total nitrogen, both showing significant positive correlations. The RDA2 axis explained 21.23% of the variation, mainly influenced by available potassium and pH with available potassium positively correlated and pH negatively correlated (Figure 7b). Whether in RS or NRS, soil physicochemical factors largely determined the structural changes of the microbial community.

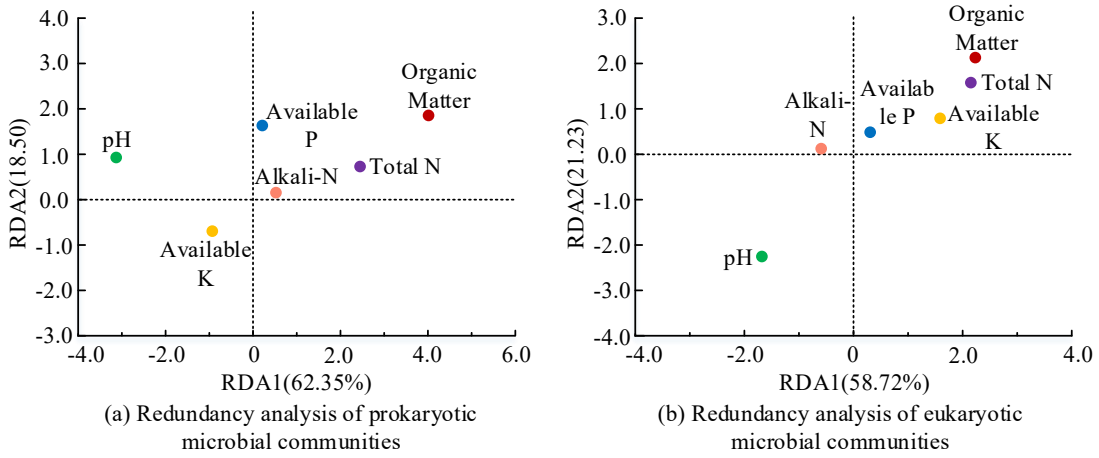

Figure 7. Redundancy analysis of microbial communities and soil physicochemical factors.

Discussion

China is a major producer of ginseng in the world. However, the traditional cultivation mode of ginseng is deforestation, which has a strong destructive effect on forest resources and causes ecological pressure [17]. To explore suitable soil for cultivating ginseng and improve ginseng yield, this study investigated the effects of cultivating ginseng on RMC structure and its interaction with pathogenic bacteria to explore the structural differences and driving mechanisms of RMC through species level abundance curves, alpha diversity, beta diversity, and differential group analysis. The results demonstrated that the ADI of PMG in RS was lower than that in NRS ($P < 0.05$), while there was no discrepancy in the ADI of EMG. The Chao1, Shannon, and phylogenetic diversity indexes of PMG in NRS were higher than that in RS. The results indicated that the rhizosphere environment had a inhibitory effect on the PMC diversity, while its impact on EMG was relatively small. Kim *et al*. also pointed out that the selective effect of root exudates in RS and the specificity of the rhizosphere microenvironment were important reasons [18]. In addition, the enriched PMG such as *Bacillales* and *Bacilli* in the RS showed significant antagonistic effects on *Cylindrocarpon destructants* and *Rhizoctonia solani*. The antibacterial effect of EMG *H. grisea* was relatively weak. In NRS, the inhibition rate of the *Zygomycota phylum* was low, and some groups even showed negative inhibition effects. The correlation matrix showed that the number of genera related to *Bacillus* and *Pseudomonas* in RS was 0.91 and 0.73, respectively, compared to the family *Trichomycteridae*. The NRS only had a correlation of 0.91 between *Ascomycota* and *Rosaceae*, while most other groups showed a negative correlation. The results indicated that the microbial community enriched in RS had a stronger inhibitory effect on pathogenic bacteria. In terms of soil physicochemical properties, the pH values of NRS samples ranged from 6.52 to 6.91, while the pH values of RS samples B1 to B5 ranged from 6.05 to 6.22. In organic matter, RS HAC, humin carbon, and WSOC were all higher than NRS with only FAC lower than NRS. In terms of nitrogen, RS showed an increase in total nitrogen and alkaline hydrolyzed nitrogen compared to NRS. In terms of phosphorus and potassium, RS showed an increase in available phosphorus compared to NRS, while available potassium decreased by at least 9.5% ($P < 0.05$) compared to NRS. The pH value of RS was generally lower than that of NRS, which might be due to the influence of rhizosphere microbial activity and root exudates, leading to increased soil acidity. The results were consistent with previous study [19]. In the correlation matrix, the correlation between RS microbial communities was relatively significant. Among them, the correlation coefficient between *Bacillales* and

Pseudomonas demonstrated a strong positive correlation, indicating that they might have close ecological connections and synergistic effects in the rhizosphere environment. The correlation coefficient between *Bacillales* and *Chaetomiaceae* showed a moderate positive correlation, suggesting that they might have a certain degree of functional complementarity or mutual assistance in the RS. In the RDA analysis of PMC, the RDA1 axis explained 62.35% of the variation, while the RDA2 axis explained 18.50% of the variation. In the RDA analysis of EMC, the RDA1 axis explained 58.72% of the variation, while the RDA2 axis explained 21.23% of the variation. The results indicated that organic matter, pH, available phosphorus and potassium were the main environmental factors driving changes in MCS. The changes in soil physicochemical factors had important regulatory effects on the distribution and diversity of different types of microbial communities, which was also confirmed by the results of Simon *et al*. [20].

Conclusion

The physicochemical properties and nutrient content of RS were significantly different from those of NRS. These differences had significant impacts on the diversity and ecological relationships of microbial communities. The PMC exhibited significant inhibitory effects in RS, while the EMC was relatively stable. The enriched microbial community in RS had a significant antagonistic effect on pathogenic bacteria. In addition, ginseng exhibited targeted selection towards RMC, significantly reducing PMG diversity but enriching beneficial groups such as *Bacillus* and *Actinobacteria* with only an increase in Shannon index for EMG. Soil physical and chemical properties were key driving factors for RMC differentiation, and they worked together with microorganisms to shape the rhizosphere disease resistant environment. The order *Bacillus* and class *Bacillus* in RS were the core groups that inhibited pathogenic bacteria with inhibition rates ranging from 76.9% to 89.2%. Their synergistic effect with the genus *Pseudomonas* further enhanced disease resistance. The research results revealed the coupling mechanism between ginseng, soil, microorganisms, and pathogens, providing a scientific basis for improving ginseng disease resistance and yield by regulating RMC. In the future, metagenomics can be combined to analyze the functional genes of key microorganisms and further improve regulatory targets.

References

1. Ito H, Ito M. 2024. Recent trends in ginseng research. J Nat Med. 78(3):455-466.
2. Fang X, Wang M, Zhou X, Wang H, Wang H. 2022. Effects of growth years on ginsenoside biosynthesis of wild ginseng and cultivated ginseng. BMC Genomics. 23(1):325-327.
3. Guo M, Shao S, Wang D, Zhao D, Wang M. 2021. Recent progress in polysaccharides from Panax ginseng CA Meyer. Food Funct. 12(2):494-518.
4. Fan S, Zhang Z, Su H, Xu P, Qi H, Zhao D, *et al*. 2020. Panax ginseng clinical trials: Current status and future perspectives. Biomed Pharmacother. 132:1-12.
5. Huang J, Wu Y, Gao Q, Li X, Zeng Y, Guo Y, *et al*. 2024. Metagenomic exploration of the rhizosphere soil microbial community and their significance in facilitating the development of wild-simulated ginseng. Appl Environ Microbiol. 90(3):2335-2340.
6. Aizi T, Lijuan L, Lihua L, Wei L, Jiamei Q. 2023. Comparative analysis of microbial community structure in different times of Panax ginseng rhizosphere microbiome and soil properties under larch forest. BMC Genomic Data. 24(1):51-57.
7. Chen G, Xue Y, Yu X, Li C, Hou Y, Zhu H, *et al*. 2022. The structure and function of microbial community in rhizospheric soil of American ginseng (*Panax quinquefolius* L.) changed with planting years. Curr Microbiol. 79(9):281-290.
8. Jang W, Jang Y, Cho W, Lee SH, Shim H, Park JY, *et al*. 2022. High-throughput digital genotyping tools for Panax ginseng based on diversity among 44 complete plastid genomes. Plant Breed Biotechnol. 10(3):174-185.
9. Tong AZ, Liu W, Liu Q, Ma GQ, Zhu JY. 2021. Diversity and composition of the Panax ginseng rhizosphere microbiome in various cultivation modes and ages. BMC Microbiol. 21(1):18-25.
10. Choi J, Kim J, Yoon HI, Son JE. 2022. Effect of far-red and UV-B light on the growth and ginsenoside content of ginseng (Panax ginseng CA Meyer) sprouts aeroponically grown in plant factories. Hortic Environ Biotechnol. 63(1):77-87.
11. Zhao S, Song W, Hou Z, Wang Z. 2021. Classification of ginseng according to plant species, geographical origin, and age using

laser-induced breakdown spectroscopy and hyperspectral imaging. J Anal At Spectrom. 36(8):1704-1711.

12. Iqbal M, Hartati H, Victorian AR. 2024. Implementation of physical fitness test measurement in basketball using an application. ACTIVE J Phys Educ Sport Health Recreat. 13(1):93-101.
13. Ji L, Tian L, Nasir F, Chang J, Chang C, Zhang J, *et al*. 2021. Impacts of replanting American ginseng on fungal assembly and abundance in response to disease outbreaks. Arch Microbiol. 203(5):2157-2170.
14. Radha Abbas Hasoon M, Jawad Kadhim N. 2021. Improvement of the selectivity index (SI) and cytotoxicity activity of doxorubicin drug by panax ginseng plant extract. Arch Razi Inst. 76(3):659-666.
15. Wang B, Li Y, Zhao J, Yang S, Wei F, Huang X, *et al*. 2021. Root rot-infected Sanqi ginseng rhizosphere harbors dynamically pathogenic microbiotas driven by the shift of phenolic acids. Plant Soil. 465(1):385-402.
16. Hou J, Li T. 2022. Effect of air endurance training on athlete's lower limb explosive strength. Rev Bras Med Esporte. 28(5):513-516.
17. Zhang YX, Niu YQ, Wang XF, Wang ZH, Wang ML, Yang J, *et al*. 2022. Phenotypic and transcriptomic responses of the shade-grown species Panax ginseng to variable light conditions. Ann Bot. 130(5):749-762.
18. Muzakky H. 2025. Kontribusi power otot lengan dan koordinasi mata–tangan terhadap hasil passing chest pass basket siswa ekstrakurikuler basket SMK Negeri 2 Teluk Kuantan. Integrative Sport J. 3(1):10-17.
19. Gryko K. 2021. Effect of maturity timing on the physical performance of male Polish basketball players aged 13 to 15 years. Sci Rep. 11(1):22019-22025.
20. Simon K, Vicent M, Addah K, Bamutura D, Atwiine B, Nanjebe D, *et al*. 2023. Comparison of deep learning techniques in detection of sickle cell disease. AIA. 1(4):252-259.